Wideband and High Quality Factor Shear Horizontal SAW Resonators with Improved Temperature Stability in LNOI Platform

Tzu-Hsuan Hsu, Kuan-Ju Tseng, and Ming-Huang Li*
Department of Power Mechanical Engineering
National Tsing Hua University
Hsinchu, Taiwan
*mhli@pme.nthu.edu.tw

***Abstract*—In this work, the relation between temperature coefficient of frequency (TCF) and wavelength (λ) of a shear horizontal surface acoustic wave (SH-SAW) resonator in lithium niobate-on-insulator (LNOI) platform is investigated numerically and experimentally. Proposed device achieves a low TCF of -18.5 ppm/K, quality factor (Q_{max}) of 1360, and effective electromechanical coupling factor (k^2_{eff}) of 21.2%, yielding a high figure-of-merit (FOM1 = $k^2_{\text{eff}} \cdot Q_{max}$) of 288. The dispersive behavior of the TCF was first analyzed based on finite element method (FEM), which reveals the strong correlation between TCF and the thickness of LN (h_{LN}) and SiO_2 (h_{SiO2}) thin films. To confirm our observations, three prototyped SH-SAW devices with λ of 2.8, 4, and 6 μm were fabricated and characterized, showing TCFs approximately -86, -45, and -18.5 ppm/K, respectively, for both series and parallel resonance frequencies. The results captured through experiments fits well with the trends predicted in the FEM simulations. Furthermore, the proposed resonator (λ = 6 μm, TCF = -18.5ppm/K, FOM1 = 288) exhibits a very competitive performance among state-of-the-art thin film LN/LT resonators.**

Keywords—temperature coefficient of frequency; wavelength, lithium niobate-on-insulator; surface acoustic wave, shear horizontal, resonator, piezoelectric

I. Introduction

As 5G wireless continues to thrive, to accommodate high data rate, RF filters inevitably need to target newer and higher frequency bands with wider bandwidth. This poses challenges for RF filters to feature increased quality factor (Q), higher electromechanical coupling factor (k^2_{eff}) and improved frequency stability to meet the ever-tighter duplex gaps and bandwidth requirements. Moreover, as the increasingly stringent band allocation requirements become mandatory for all RF filters to meet [1], the importance of temperature stability has then played an important role among the resonator and filter design.

In recent years, a new class of surface acoustic wave (SAW) devices base on *thin film* lithium tantalate or lithium niobate on insulators (LTOI [2]/LNOI [3]) has attracted numerous research interests as they feature high Q and larger coupling due to the elimination of bulk acoustic wave radiation towards substrate [4]. By forming a hetero acoustic impedance layer with a SiO_2 thin film underneath the LN/LT, the guided shear horizontal SAW (SH-SAW) wave is confined at the surface of wafer. In our previous work, a high-performance SH-SAW resonator has been demonstrated by X-cut LNOI with LN and SiO_2 thickness of 0.7 and 2 μm, respectively, showing a high-k^2_{eff} of 25.5% and Q of 960 around 580 MHz. However, the temperature coefficient of frequency (TCF) of such devices are rarely discussed.

Therefore, in this work, we attempt to investigate the temperature characteristics of SH-SAW under various thin film thicknesses and to develop low-TCF devices targeting wideband and high Q in LNOI.

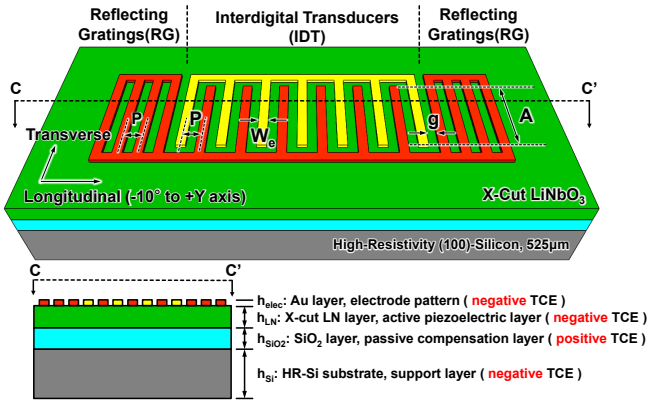

Fig. 1. Mock-up view of the LNOI SH-SAW resonator used to investigate the temperature stability with key design parameters.

II. Device Design and Simulation

A. Resonator Design and Temperature Compensation

To investigate the temperature stability of acoustic devices designed in LNOI platform [5], the one-port SH-SAW resonator with synchronous placement of the interdigital transducers (IDT) was implemented, as shown in Fig. 1. The SiO_2 underneath the active piezoelectric layer served as a passive temperature compensation layer. In our design, the IDT pitch (P) was set as λ/2 while the electrode width (W_e), and the IDT-reflecting gratings gap (g) were both λ/4 wide. The aperture (A) was fixed at 20λ. To enhance the effective electromechanical coupling of the SH-SAW based on thin

This work is sponsored through the Young Scholar Fellowship Program of Ministry of Science and Technology of Taiwan (MOST 109-2636-E-007-023).

978-1-6654-3935-0/21/$31.00 ©2021 IEEE

TABLE I. MATERIAL PROPERTIES ADOPTED IN THIS WORK

Parameter	Symbol	Z-Cut $LiNbO_3$ (TC, ppm/K)	Au (TC, ppm/K)	SiO2 (TC, ppm/K)	Si (TC, ppm/K)
Elastic stiffness (constant electric field) [GPa]	c_{11}^E	203 (-174)	E = 70 (-200) v = 0.44 Isotropic	E = 72 (185) v = 0.17 Isotropic	166 (-73.25)
	c_{12}^E	57.3 (-252)			64 (-91.59)
	c_{13}^E	75.2 (-159)			64 (-91.59)
	c_{14}^E	8.5 (-214)			0
	c_{33}^E	242.4 (-153)			166 (-73.25)
	c_{44}^E	59.5 (-203)			80 (-60.14)
	c_{66}^E	72.8 (-143)			80 (-60.14)
Piezoelectric stress constants [C/m²]	e_{15}	3.76 (147)	–	–	–
	e_{22}	2.43 (79)	–	–	–
	e_{31}	0.23 (221)	–	–	–
	e_{33}	1.33 (887)	–	–	–
Relative permittivity (constant strain)	ε_{11}^S	43.6 (323)	–	3.9	9
	ε_{33}^S	29.16 (627)	–	3.9	9
Density [kg/m³]	ρ	4700	19300	2200	2330

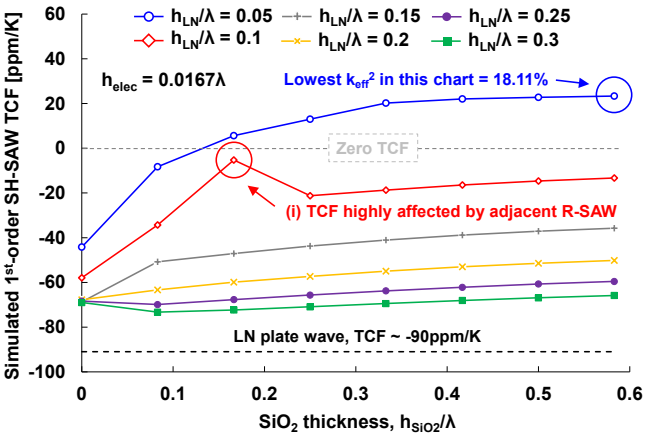

Fig. 2. Simulated 1st-order TCF of the LNOI SH-SAW resonators under normalized h_{LN}/λ and h_{SiO2}/λ ratios.

metal electrodes, the X-cut LN thin film was selected as the piezoelectric layer [6] with heavy metals (Au) as the IDT electrode. The TCF of an arbitrary acoustic resonator is attributed to the variations in acoustic velocity and the dimension of the resonator with temperature. In general, the 1st-order TCF can be approximated as:

$$TCF = \frac{1}{f(T_0)}\frac{df(T)}{dT} \approx TCF^V + TCF^\alpha, \quad (1)$$

where TCF^V and TCF^α denotes the TCF corresponding to the acoustic wave velocity and the thermal expansion coefficient, respectively. In a typical case, the overall TCF is predominantly governed by TCF^V [7].

For an SH-SAW resonator in LNOI platform, the acoustic energy is largely confined in the LN/SiO_2 composite stack during operation. Considering the LN and SiO_2 feature opposite temperature coefficient of velocities (negative TCF^V for LN and positive TCF^V for SiO_2), it is possible to achieve a near-zero TCF based on an optimal LN/SiO_2 thickness ratio. Since the energy distribution profile, the relative metal thickness, and the relative LN thickness of the SH-SAW are different when λ (i.e., IDT pitch) is different, the TCF becomes λ-dependent in a fixed LN/SiO_2 ratio.

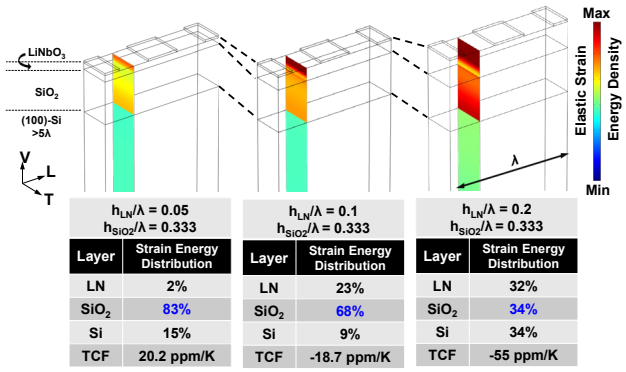

h_{LN}/λ = 0.05, h_{SiO2}/λ = 0.333	
Layer	Strain Energy Distribution
LN	2%
SiO_2	83%
Si	15%
TCF	20.2 ppm/K

h_{LN}/λ = 0.1, h_{SiO2}/λ = 0.333	
Layer	Strain Energy Distribution
LN	23%
SiO_2	68%
Si	9%
TCF	-18.7 ppm/K

h_{LN}/λ = 0.2, h_{SiO2}/λ = 0.333	
Layer	Strain Energy Distribution
LN	32%
SiO_2	34%
Si	34%
TCF	-55 ppm/K

Fig. 3. Strain energy distribution based on different h_{LN} ratios with h_{SiO2}/λ set as constant. Note that the total strain energy for each case was not the same.

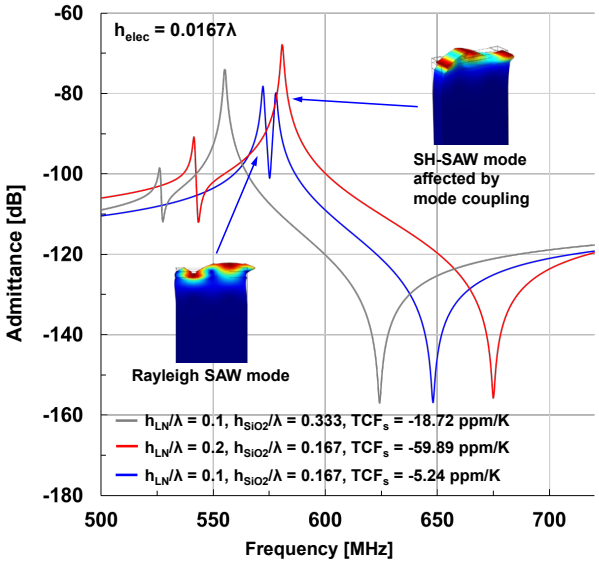

Fig. 4. Simulated frequency spectrum with adjacent mode coupling under certain h_{LN}/λ and h_{SiO2}/λ ratios.

B. *Linear TCF Simulation By FEM*

To extract the 1st-order TCF of the LNOI SH-SAW with various LN/SiO_2 ratios, a 3D periodic unit cell (PUC) model was used in conjunction with COMSOL Multiphysics [8]. The material properties used in the simulation are tabulated in Table I [9]-[11], and the detailed simulation setup can be found in [6].

Fig. 2 illustrates the simulated TCFs based on thin Au electrodes with h_{elec} = 0.0167λ. The TCF of the SH_0 plate wave in X-cut LN is also plotted on the same figure for comparison, which is around -90 ppm/K. As h_{LN}/λ decreases from 0.3 to 0.05, the TCF of SH-SAW changes from negative to positive. It is observed that near-zero TCF is possible under certain h_{LN}/λ and h_{SiO2}/λ combinations ($h_{LN}/\lambda \approx 0.05$ and $h_{SiO2}/\lambda \approx 0.14$). Moreover, the simulation shows that the k_{eff}^2 becomes smaller at higher h_{SiO2}/λ, since more acoustic energy is confined in SiO_2 instead of LN. Fortunately, the lowest k_{eff}^2 of 18.11% for an over-compensated resonator ($h_{LN}/\lambda \approx 0.05$ and $h_{SiO2}/\lambda \approx 0.58$)

TABLE III. LNOI SH-SAW DESIGN PARAMETER USED IN THIS WORK

Parameters	Values	Unit
h_{LN}	0.7	μm
h_{SiO2}	2	μm
h_{elec}	0.1	μm
Wavelength (λ)	2.8, 4, 6	μm
Aperture	20	λ
number of IDT Pairs	40	-
number of RGs	20 fingers per side	-
Electrode width (W_e)	1/4	λ
IDT-RG Gap (g)	1/4	λ

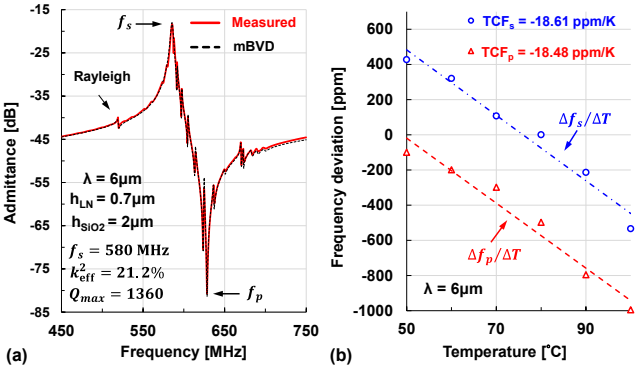

Fig. 5. (a) LNOI SH-SAW resonator frequency response measured under room temperature. (b) Measured frequency drift of both f_s and f_p based on the device in Fig. 5(a).

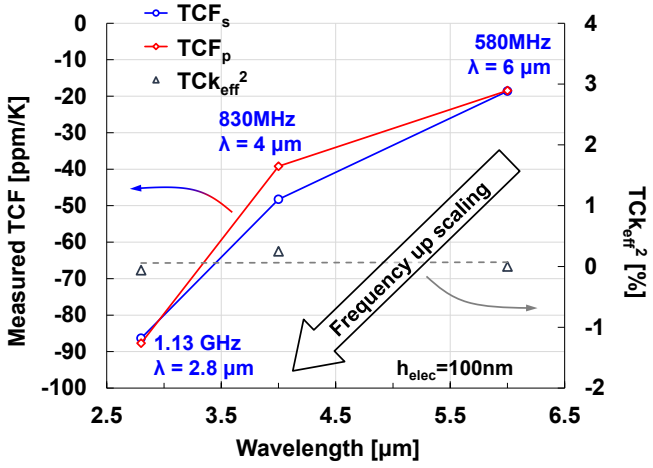

Fig. 6. Measured TCF and TCk^2_{eff} regarding different resonator wavelengths covering multiple h_{LN}/λ and h_{SiO2}/λ ratios.

among all data points shown in this figure is still sufficient for wideband filtering applications.

To explain the trend of the simulated TCFs in Fig. 2, the strain energy distribution in thickness direction under different h_{LN}/λ was depicted in Fig. 3 (fixed h_{SiO2}/λ=0.333). In this PUC model, the SH wave propagates along the longitudinal (L) axis while the particle motion is along the transverse (T) axis. Based on the simulation results, the TCF compensation capability of LNOI topography is highly influenced by the strain energy distribution across LN and SiO_2 layers. For smaller h_{LN}/λ, the strain energy tends to concentrate in the SiO_2 layer to shift the TCF towards positive side and vice versa.

In addition, for specific h_{LN}/λ and h_{SiO2}/λ ratios, the 1st-order TCF is highly affected by adjacent Rayleigh-SAW (R-SAW) mode, as indicated by (i) in Fig. 2. To further identify the cross correlation between R-SAW and SH-SAW, the frequency responses at different h_{LN}/λ and h_{SiO2}/λ are depicted in Fig. 4. At the point of interest (point (i), $h_{LN}/\lambda \approx 0.1$ and $h_{SiO2}/\lambda \approx 0.167$), the R-SAW mode is acoustically coupled with the SH-SAW mode. Although the TCF is significantly lowered at this point, the dual resonance peak behavior is not desired in many practical applications.

TABLE II. COMPARISON OF THIN FILM LN/LT RESONATORS.

	This work	JMEMS'15 [13]	JMEMS'19 [9]	JMEMS'20 [14]	IUS'17 [2]
Device Type	LNOI	TF LN	TF LN/SiO_2	LNOI	LT-Quartz
Crystal Cut	X-LN	136°-Y LN	36°-Y LN	X-LN	20°YX-LT
Acoustic Mode	SH-SAW	S_0 Lamb	SH_0 Overtone	SH-SAW	SH-SAW
$h_{LN/LT}$ [μm]	0.7	1	0.7	1	1.12
h_{SiO2} [μm]	2	--	2	1	--
Metallization	Au	Au	Al	AlSi	Cu
h_{elec} [nm]	100	80	200	300	480
λ [μm]	6	11.2	11	6.7	7.76
f_s [MHz]	580	513	340*	580*	450*
k^2_{eff} [%]	21.2	14.5*	3	22*	12.3+
**BW [%]	8.27	5.88+	1.2	8.9+	5.0
Bode-Q (Q_{max})	1360	960	3300	1350*	3000
TCF [ppm/K]	-18.5	-84	+10	-30	-26
FOM1 = $k^2_{eff} \cdot Q_{max}$	288	140	99	297	369
FOM2 = BW · Q_{max}	112	57	39	120	150

+Estimated by $k^2_{eff} \approx (\pi^2/4) \cdot BW$ or $BW \approx (4/\pi^2) \cdot k^2_{eff}$
*Extracted from the figures provided in the corresponding manuscript

III. EXPERIMENTAL RESULTS

A. Fabrication Process

The LNOI wafer adopted in this work was sorted externally through commercial vendors. The wafer was fabricated based on the smart-cut process. The IDT patterns were defined through an in-house single electron beam (E-beam) lithography. Then the Au IDT electrodes was defined by a standard lift-off process. The resonator dimensions are summarized in Table II. The h_{LN} and h_{SiO2} selected in this work were 0.7 and 2 μm, respectively.

B. Measurement setup

To extract the TCF of the LNOI SH-SAW resonators, the SH-SAW devices were characterized with a vector network analyzer (Keysight E5071C) and GSG probes in ambient pressure. For the temperature stability experiment, a customized probe station with a built-in heater and PID temperature controller was used to control the temperature of the resonator. The temperature range measured in this work is from 40°C up to 100°C. At each data point, the chip temperature was stabilized for at least 15 minutes to avoid unwanted transient responses. Finally, the TCF is calculated by extracting the frequency shift of both series (f_s) and parallel (f_p) resonance from the converted admittance plot (Y_{11}) at different temperatures.

C. Measurement results

The measured responses are fitted through a multi-resonance modified Butterworth-Van Dyke (mBVD) model. Fig. 5(a) shows the measured and fitted admittance of an SH-SAW resonator at 580 MHz (λ = 6 μm), showing a k^2_{eff} of 21.2% and a maximum Bode-Q of 1360. The TCF at series (TCF_s) and parallel (TCF_p) resonant frequencies of this device are extracted in Fig. 5(b). Noted that the measured TCF_s = -18.61 ppm/K and TCF_p = -18.48 ppm/K is comparable to commercially available TCSAW devices [12].

We further investigate the resonator's TCF across different wavelengths based on the same wafer. The temperature stability of the SH-SAW resonators at different wavelength (λ = 2.8, 4, and 6 μm) is summarized and compared in Fig. 6, showing a minimum TCF of -18.5 ppm/K (λ = 6μm) and maximum TCF of -87 ppm/K (λ = 2.8μm), respectively. Those short-wavelength designs (λ = 2.8 and 4 μm) reveals that the passive compensation becomes less effective as explained in Sec. II-B. Finally, no apparent temperature coefficient of electromechanical coupling factor (TCk^2_{eff}) was observed during our experiment across different wavelength designs since the $\Delta TCF = TCF_s - TCF_p$ is small. This is a desired property for wideband filters.

A comparison of our work with the state-of-the-art thin-film LN/LT piezoelectric resonators is shown in Table III [2][9][13][14]. Given the high FOM1 of 288 and the low TCF of -18.5 ppm/K, the proposed SH-SAW resonator is a potential candidate for high-performance RF front-end applications.

IV. Conclusions

In this work, the passive temperature compensation scheme of SH-SAW devices was investigated in LNOI platform. By carefully controlling the thickness of SiO_2, near-zero TCF is conceptually achievable under certain combinations of h_{LN}/λ and h_{SiO2}/λ. The measured admittance response of a prototyped resonator (λ = 6μm) with thin Au electrodes of 100 nm exhibits a minimum TCF of -18.5 ppm/K at both f_s and f_p. Measured TCFs adhered with the trend predicted in FEM simulation well, where the temperature compensation becomes less effective for short-wavelength devices (i.e., larger h_{LN}/λ).

Acknowledgment

The authors would like to thank the Young Scholar Fellowship Program of Ministry of Science and Technology of Taiwan (MOST 109-2636-E-007-023) for funding support, and the CNMM of National Tsing Hua University and the Taiwan Semiconductor Research Institute (TSRI) for device fabrication. The authors would also acknowledge Mr. Chin-Yu Chang at National Tsing Hua University and Prof. Wei-Chang Li at National Taiwan University for helpful discussions and TCF measurement assistance.

References

[1] Y. Hori, H. Kobayashi, K. Tohyama, Y. Iwasaki and K. Suzuki, "A hybrid substrate for a temperature-compensated surface acoustic wave filter," *in Proc. IEEE Ultrason. Symp. (IUS)*, Sept. 2009, pp. 2631-2634.

[2] M. Kadota and S. Tanaka, "Improved quality factor of hetero acoustic layer (HAL) SAW resonator combining LiTaO3 thin plate and quartz substrate," *in Proc. IEEE Ultrason. Symp. (IUS)*, Sept. 2017, pp. 1-4.

[3] T.-H. Hsu, K. -J. Tseng and M. -H. Li, "Large coupling acoustic wave resonators based on $LiNbO_3/SiO_2/Si$ functional substrate," *IEEE Electron Device Lett.*, vol. 41, no. 12, pp. 1825-1828, Dec. 2020.

[4] S. Inoue and M. Solal, "Spurious free SAW resonators on layered substrate with ultra-high Q, high coupling and small TCF," *in Proc. IEEE Ultrason. Symp. (IUS), Oct. 2018*, pp. 1-9.

[5] T.-H. Hsu, F.-C. Su, K.-J. Tseng, and M.-H. Li, "Low loss and wideband surface acoustic wave devices in thin film lithium niobate on insulator (LNOI) platform," in *Proc., 34th IEEE Micro Electro Mechanical Systems (MEMS'21)*, Jan. 2021, pp. 474-477.

[6] T.-H. Hsu, K.-J. Tseng and M.-H. Li, "Thin-film lithium niobate-on-insulator (LNOI) shear horizontal surface acoustic wave resonators," *J. Micromech. Microeng.*, , vol. 31, no. 5, pp. 054003, May 2021.

[7] C.-M. Lin, T.-T. Yen, Y.-J. Lai, V. Felmetsger, M. Hopcroft, J. Kuypers, and A. Pisano., "Temperature-compensated aluminum nitride Lamb wave resonators," *IEEE Trans. on Ultrason., Ferroelectr., Freq. Control*, vol. 57, no. 3, pp. 524-532, Mar. 2010.

[8] (Available at: www.comsol.com)

[9] M.-H. Li, C.-Y. Chen, R. Lu, Y. Yang, T. Wu, and S. Gong, "Temperature stability analysis of thin-film lithium niobate SH0 plate wave resonators," *J. Microelectromech. Syst.*, vol. 28, no. 5, pp. 799-809, Oct. 2019.

[10] A. Ansari and M. Rais-Zadeh, "A temperature-compensated gallium nitride micromechanical resonator," *IEEE Electron Device Lett.*, vol. 35, no. 11, pp. 1127-1129, Nov. 2014.

[11] M. A. Hopcroft, W. D. Nix and T. W. Kenny, "What is the Young's Modulus of Silicon?," *J. Microelectromech. Syst.*, vol. 19, no. 2, pp. 229-238, Apr. 2010.

[12] Qorvo, "Redefining filter performance", 2018 (Available at: https://www.qorvo.com/resources/d/qorvo-advanced-filtering-solutions-brochure)

[13] R. Wang, S. A. Bhave, and K. Bhattacharjee, "Design and fabrication of S0 Lamb-wave thin-film lithium niobate micromechanical resonators," *J. Microelectromech. Syst.*, vol. 24, no. 2, pp. 300-308, Apr. 2015.

[14] A. Kochhar, A. Mahmoud, Y. Shen, N. Turumella and G. Piazza, "X-Cut lithium niobate-based shear horizontal resonators for radio frequency applications," *J. Microelectromech. Syst.*, vol. 29, no. 6, pp. 1464-1472, Dec. 2020.